Published in final edited form as:
Cell Mol Bioeng. 2013 December ; 6(4): 441–448. doi:10.1007/s12195-013-0295-6.

Lineage tracing quantification reveals symmetric stem cell division in Drosophila male germline stem cells

Viktoria Salzmann[1], **Mayu Inaba**[1], **Jun Cheng**[2,*], and **Yukiko M. Yamashita**[1,*]

[1]Life Sciences Institute, Department of Cell and Developmental Biology, University of Michigan Ann Arbor

[2]Department of Bioengineering, University of Illinois at Chicago, 851 S Morgan Street, Chicago IL 60607

Summary

In the homeostatic state, adult stem cells divide either symmetrically to increase the stem cell number to compensate stem cell loss, or asymmetrically to maintain the population while producing differentiated cells. We have investigated the mode of stem cell division in the testes of *Drosophila melanogaster* by lineage tracing and confirm the presence of symmetric stem cell division in this system. We found that the rate of symmetric division is limited to 1-2% of total germline stem cell (GSC) divisions, but it increases with expression of a cell adhesion molecule, E-cadherin, or a regulator of the actin cytoskeleton, Moesin, which may modulate adhesiveness of germ cells to the stem cell niche. Our results indicate that the decision regarding asymmetric vs. symmetric division is a dynamically regulated process that contributes to tissue homeostasis, responding to the needs of the tissue.

Introduction

Adult stem cells play a fundamental role in tissue homeostasis through the continuous production of differentiated cells. The balance between stem cell self-renewal and commitment to differentiation is crucial for long-term maintenance of tissue homeostasis. Asymmetric stem cell division, which produces one stem cell and one differentiating cell, has proven to be a vital mechanism to achieve this balance.

Although it has been postulated that stem cells maintain their identity stably, recent studies have revealed the dynamic nature of stem cell maintenance. In male and female germline stem cells (GSCs) in *Drosophila*, dedifferentiation or reversion of partially differentiated cells was reported to contribute to maintenance of stem cell number [1-4]. Mouse spermatogonial stem cells have been reported to undergo symmetric divisions, and the decision of self-renewal vs. differentiation is suggested to be stochastic [5-7]. The stochastic mode of stem cell self-renewal is also reported in mouse intestinal stem cells [8,9]. With these new insights, the distinction between stem cells and differentiating daughter cells has become less clear. If committed progenitor cells can revert to stem cell identity, why do stem cells have to develop a mechanism to ensure asymmetric stem cell division? And how strictly is the asymmetric outcome of stem cell division regulated?

Drosophila male GSCs have served as a premier model system to study asymmetric stem cell division. GSCs are identifiable at a single cell resolution in normal tissue anatomy,

Author for correspondence: yukikomy@umich.edu and juncheng@uic.edu.

Authors declare no conflict of interest

where GSCs attach to a cluster of post-mitotic hub cells with adherens junctions (Figure 1). Hub cells, together with cyst stem cells, provide a critical signaling microenvironment that specifies GSC identity [10-13]. Upon GSC divisions, the daughter cells that maintain the attachment to the hub cells retain stem cell identity, whereas the daughter cells that are displaced away from the hub initiate a differentiation program. We have previously shown that the asymmetric outcome of the GSC division is controlled by spindle orientation perpendicular to the hub cells (Figure 1) [14]. Such stereotypical spindle orientation is prepared by precise centrosome positioning during interphase [15]. Although we have postulated that GSCs undergo asymmetric stem cell division with almost 100% accuracy, based on the observation that spindle misorientation is extremely rare in wild-type GSCs, Sheng and Matunis recently showed that about 7% of GSCs undergo symmetric self-renewal division, despite oriented spindles: the GSC daughter that is displaced away from the hub was observed to "crawl back" to regain the attachment to the hub cells, becoming GSCs [16]. At the same time, they also observed 13% of cases of symmetric differentiation, where both daughters of GSC division lose the attachment to the hub and initiate differentiation.

In this study, we examined the frequency of symmetric stem cell divisions using an independent method and found that GSCs indeed undergo symmetric stem cell division at a certain rate, albeit at a slightly lower rate than previously reported. Furthermore, our quantitative results show that the rate of symmetric stem cell division is modulated by the expression levels of E-cadherin and Moesin in germ cells.

Results and Discussion

Recently, Sheng and Matunis reported that *Drosophila* male GSCs undergo frequent symmetric self-renewal and symmetric differentiation [16]. Using live observation, they showed that, although GSC mitotic spindles are consistently oriented perpendicular to the hub cells, the differentiating daughter (gonialblast; GB), which was displaced away from the hub, "crawls back" to adhere to the hub cells after the division, resulting in two self-renewing GSCs (termed "symmetric self-renewal"). Such symmetric self-renewal was observed in 7% of GSC divisions. The symmetric self-renewal is apparently counter-balanced by GSC divisions, wherein both daughters of GSC division lose the attachment to the hub cells, leading to stem cell loss (termed "symmetric differentiation"). Such stem cell loss was observed in 13% of GSC divisions.

Consistent with this observation, examination of fixed samples revealed the presence of two GSCs that are connected by a contractile ring and cytoplasmic bridge (Figure 2A). This presumably reflects the event wherein a GB gained attachment to the hub, resulting in symmetric self-renewal. Consistently, the cytoplasmic bridge between the cells (arrow, Figure 2A) was observed distal from the hub cells, suggesting that the site of cytokinesis originally occurred away from the hub cells, and then a GB crawled back to adhere to the hub cells. The frequency of such occurrence was somewhat lower (approximately 2% of all GSC-GB pairs, n>200 GSCs, from multiple genetic backgrounds) than that reported by Sheng and Matunis (7%). It is possible that the cytoplasmic bridge between two GSCs is quickly resolved, and therefore, escapes detection, leading to our estimation of 2%. Alternatively, experimental conditions performed by Sheng and Matunis might result in a somewhat higher frequency of symmetric divisions: 7% of symmetric self-renewal, 13% of symmetric differentiation and 0% of dedifferentiation as reported by Sheng and Matunis would lead to significant GSC loss (reduced by half in 10 cell cycles, corresponding to ~5 to 7 days based on a 12- to 16-hour cell cycle [17]). However, it is known that the GSC number is maintained relatively well in vivo (~9 GSCs per testis at newly eclosed flies and ~8 GSCs at day-30 old flies)[3,18,19].

Therefore, we sought an independent method to measure the frequencies of symmetric self-renewal. To this end, we developed transgenic flies in which GFP-positive GSC clones can be induced upon expression of FLP recombinase (Figure 2B). FLP expression will remove the mCherry ORF and stop codon from nos-FRT-mCherry-stop-pA-FRT-gal4, UAS-GFP, leading to expression of nos-gal4. The expression of nos-gal4 in turn drives the expression of UAS-GFP, labeling the clones. We combined this transgene with heat shock (hs)-FLP to induce a clone in a temporarily controlled manner. Although mCherry was introduced to positively mark the cells without FLP-mediated recombination, the mCherry signal was too weak for practical use: thus, we primarily used GFP for identification of cells that underwent FLP-mediated recombination, and the lack of GFP for identification of cells that did not undergo FLP-mediated recombination. The advantage of this system is the ability to drive the expression of additional transgenes selectively in the recombined clones by nos-gal4 (see below).

Using this system, the behavior of GSC clones can be tracked. If a GFP^+ GSC undergoes symmetric self-renewal, it would lead to two GFP^+ GSCs that are juxtaposed to each other (Figure 2C, D, E, “doublet”). Conversely, if a GFP^+ GSC undergoes symmetric differentiation, the GFP^+ GSC clone will be lost. If the GFP^+ GSC undergoes asymmetric division, it will remain as a single GFP^+ GSC (“singlet”). By scoring the changes in the frequencies of singlets and multiplets (e.g., doublets and triplets), the frequencies of asymmetric and symmetric divisions can be calculated.

We optimized the heat shock time to 30 min at 37°C. Under this condition, after 24 hours post heat shock (when GFP expression becomes reliably detectable), we observed that approximately 7% of total GSCs were GFP^+ (214 GFP^+ GSCs were observed out of 357 testes. Note that a small population of testes contained multiple clones). Without heatshock, GFP^+ clone was never observed (n>500 testes), suggesting that all GFP clones are generated by heatshock treatments at the time of heatshock. Upon heatshock treatment at 37°C for 30 min, 46% of testes contained clone(s), and the rest (54%) contained no clones (n=357 control testes examined). When the testes contained clones, 90% of GSC clones existed as singlets, 8% as doublets, and 2% as triplets (singlets, doublets, and triplets are defined in Figure 2C, D). Since each GSC would undergo one or two divisions within the first 24 hours (based on 12–16 hours of cell cycle time reported in a previous study [17]), at least some of the multiplets observed at 24 hours likely reflect symmetric self-renewal. This was taken into account in our simulation (see below). This heat shock condition was chosen to maximize the frequency of clone induction, yet minimize the occurrence of “accidental multiplets” due to independent recombination events in juxtaposed GSCs.

We simulated how GSC clones would behave as they undergo various stem cell divisions (namely, asymmetric stem cell division, symmetric self-renewal and symmetric differentiation). We assumed that the frequency of symmetric self-renewal and differentiation is equivalent because we do not observe net loss of GSC numbers in the early stages of *Drosophila* adulthood. Based on this model, the distribution of GSC clones (as singlets or multiplets) was simulated as GSCs divide (Figure 3). If the frequency of symmetric self-renewal is zero, the frequencies of singlets and multiplets remain constant over time (Figure 3A). As the frequency of symmetric self-renewal becomes higher, the multiplets will expand faster over time (Figure 3B-D). At the rate of 5% symmetric self-renewal (and counter-balancing with 5% symmetric differentiation), the frequency of multiplets increased considerably during the chase time, and in five cell cycles, approximately half of the total GFP^+ GSC clones will be multiplets (Figure 3D).

Using the nos-FRT-mCherry-stop-pA-FRT-gal4 UAS-GFP system, we chased the change in the frequencies of singlets, doublets, and triplets for 72 hours after clone induction. When

wild-type GSC clones were followed, the frequency of multiplets increased slightly, and up to 25% of GSC clones became multiplets after 72 hours of chase (Figure 4A). This is consistent with the idea that GSCs undergo symmetric self-renewal at a certain frequency. When the data were fitted to simulation, it was calculated that 1.3-1.9% of total GSC divisions were symmetric self-renewal (and equivalent frequencies of symmetric differentiation) (Table 1; if the cell cycle time is 12 hours, the rate of symmetric self-renewal would be 1.3%, whereas if the cell cycle time is 16 hours, the rate of symmetric self-renewal would be 1.9%. Our simulation used the assumption that, during the first 24 hours, GSC divisions would happen at the same rate (the same frequencies of symmetric renewal, symmetric differentiation and asymmetric divisions) as 24-72 hours.

These calculated frequencies of symmetric self-renewal are somewhat lower than the published report in which GFP-Moesin (Moe) or the GFP-Moesin Acting-binding domain (GMA) was used to visualize germ cells during time-lapse imaging [16]. Because Moesin is a known regulator of actin cytoskeleton, which could influence cell adhesion and/or cell migration, we tested whether expression of Moesin or GMA in GFP^+ clones may influence the behavior of GSC clones during the chase time. Expression of Moe or GMA in GFP^+ GSC clones considerably increased the frequency of multiplets (Figure 4B, C). When these results were fitted to simulation, Moe-expressing and GMA-expressing GSCs were calculated to undergo symmetric self-renewal at the frequency of 3.0-3.8% and 3.7-4.8%, respectively (Table 1). We hypothesize that expression of Moe or GMA changes cell migration and/or adhesion of GBs, leading to a higher frequency of symmetric self-renewal. Consistent with this idea, expression of DE-Cadherin-GFP (DEFL) in clones also resulted in a higher frequency of symmetric self-renewal (Figure 4D and Table 1). These data suggest that either the strength of cell adhesion or cell migration influences the outcome of GSC divisions. This may represent an underlying mechanism for GSC competition for niche occupancy [20].

Taken together, our results confirm the occurrence of symmetric GSC divisions, where a GB crawls back to the niche, leading to symmetric self-renewal. Our results show, however, the frequency of symmetric self-renewal is low and thus asymmetric stem cell division is a dominant mode of GSC divisions (~97%). In our simulation, we assumed that dedifferentiation of spermatogonia, which can potentially compensate stem cell loss and may skew our simulation, is negligible during the time period of our experiments based on the following reasons. First, during the live observation experiments by Sheng and Matunis using unperturbed testes (i.e. testes from young, well-fed adults), no occasion of dedifferentiation was observed, suggesting that it is low frequency events. This is consistent with our earlier observation that only ~5% of total GSCs were found to be the result of dedifferentiation in young males [3]. Since the observed number (~5%) of dedifferentiated GSCs is a result of cumulation through the development (i.e. 10 days, corresponding to at least 15 cell cycles by the time of observation), the frequency of dedifferentiation in several cell cycles is expected to be extremely low (at most 0.3% of dedifferentiation events /GSC cell cycle, which is at least 5-fold lower than symmetric self-renewal).

We also showed that the decision regarding asymmetric vs. symmetric divisions is influenced by expression levels of Moesin or E-cadherin, suggesting that cell adhesion or migration might be a key determinant of the mode of GSC divisions. It is to be determined whether those cells that crawled back to the niche are equally functional as bona fide GSCs. The mother/daughter centrosomes [15] as well as sister chromatids of X and Y chromosomes [21] are segregated asymmetrically during GSC divisions. Therefore, those cells that crawled back to the niche have inherited the daughter centrosome, and the sister chromatids that were destined to GBs. Future investigation is required to address whether GBs that crawled back to the niche may be different from native GSCs.

Materials and Methods

Fly husbandry and strains

All fly stocks were raised in standard Bloomington medium at 25°C. The following fly stocks were used: UAS-Moe-GFP [22], UAS-GMA, UAS-DEFL, hsFLP; nos>stop>gal4 UAS-GFP, and Pavarotti (Pav)-GFP [23].

Immunofluorescence staining

Immunofluorescence staining was performed as described previously [3]. In brief, testes were dissected in phosphate-buffered saline (PBS), transferred to 4% formaldehyde in PBS, and fixed for 30–60 minutes. The testes were then washed in PBST (PBS + 0.1% Tween 20) for >30 minutes, followed by incubation with primary antibody in 3% bovine serum albumin (BSA) in PBST at 4°C overnight. Samples were washed for 60 minutes (three 20-minute washes) in PBST, incubated with secondary antibody in 3% BSA in PBST at 4°C overnight, washed for 60 minutes (three 20-minute washes) in PBST, and mounted in VECTASHIELD with DAPI. The primary antibodies used were: mouse anti-Adducin-like (1:20, developed by H. D. Lipshitz and obtained from Developmental Studies Hybridoma Bank (DSHB)), rat anti-Vasa (1:40; developed by A. C. Spradling and D. Williams, and obtained from DSHB), mouse anti-Fasciclin III (1:50; developed by C. Goodman, and obtained from DSHB), mouse anti-gamma tubulin (1:200, SIGMA), rabbit anti-Vasa (1:200, Santa Cruz Biotechnology). Images were taken using a Leica TCS SP5 confocal microscope with a 63× oil immersion objective (NA = 1.4) and processed using Adobe Photoshop software.

Molecular cloning (construction of nos-FRT-mCherry-FRT-gal4-VP16)

Step 1: Construction of FRT-mCherry-SV40-FRT. mCherry cDNA was amplified using primers NheI mCherry Fw (5’-acgctagctatggtgagcaagggcgaggag-3’) and XhoI mCherry Rv (5’-gactcgagttacttgtacagctcgtccat-3’) from pmCherry Vector (Clontech), and then the product was introduced into NheI-XhoI sites of the pFRT-SV40-FRT vector (Gift from Elizabeth R. Gavis). A second amplification was performed using primers NdeI FRT Fw (5’-atcatatgggggatcttgaagttcctatt-3’) and XhoI mCherry Rv (5’-gactcgagttacttgtacagctcgtccat-3’), and then the product was introduced into the pGEM-T vector (Promega).

Step 2: The SV40 polyA-FRT fragment was amplified from the pFRT-SV40-FRT vector using the primers XhoI SV40 Fw (5’-gactcgagggtacctctagaggatctttgtga-3’) and NotI-NdeI-FRT Rv (5’-atgcggccgccatatgcaaaagcgctctgaagttcctatact-3’), and then the product was introduced into the XhoI-NotI site of the mCherry plasmid described in step 1.

Step 3: EGFP cDNA was amplified from pEGFP-N3 (Clontech) using the following primers: EcoRI-5’EGFP-Fw (5’-tcgaattccatcgccaccatggtgagcaa-3’) and BglII-3’RGFP-Rv (5’-tacagatctcttgtacagctcgtccatgccga-3’), and then the product was cloned into BglII-EcoRI sites of pUAST-attB [24]

Step 4: The NotI-flanked 3.13-Kb fragment from the pCSpnosFGVP (Gift from Elizabeth R. Gavis) containing the Nanos 5’ region-ATG (NdeI-start codon) Gal4-VP16-Nanos 3’ region was subcloned into two NheI sites of pUAST-EGFP-attB (described in step 3).

Step 5: The NdeI-flanked pFRT-mCherry-SV40 polyA -FRT fragment (from B) was subcloned into the NdeI start codon of the plasmid described in Step 4.

A transgene was introduced into the Basler strain (#24482) using PhiC31 integrase-mediated transgenesis systems [25] by BestGene, Inc.

Simulation of GFP$^+$ clones during GSC divisions

At each cell cycle, the probabilities of single and multiple GFP$^+$ GSCs are calculated by simulating divisions with various dividing frequencies for every GFP$^+$ GSC. The simulation algorithm is implemented in Matlab code (MathWorks Inc.). To simplify discussion, the frequency of asymmetric division is denoted as f_{as}, the frequency of symmetric self-renewal division as f_{ss}, and the frequency of symmetric differentiation as f_{sd}. At cell cycle n after heat shock, the rate of singlet GFP$^+$ GSC is $p1_n$, doublet is $p2_n$, triplet is $p3_n$, and etc. The next cell cycle, $n + 1$, the rate of singlet $p1_{n+1}$ can be calculated as

$$p1_{n+1}=p1_n * f_{as}+p2_n * 2 * f_{as} * f_{sd}+p3_n * 3 * f_{as} * f_{sd}^2+\cdots$$

where the first term on the right side is a contribution from $p1_n$, the second term is contribution from $p2_n$, third term is contributions from $p3_n$, and ⋯ represents contributions from more than 3 juxtaposed GFP$^+$ GSCs. Similarly, the rate of doublet $p2_{n+1}$ can be calculated as

$$p2_{n+1}=p1_n * f_{ss}+p2_n * \left(f_{as}^2+2 * f_{ss} * f_{sd}\right)+p3_n * 3 * \left(f_{as}^2 * f_{sd}+f_{ss} * f_{sd}^2\right)+\cdots$$

and the rate of triplet $p3_{n+1}$ can be calculated as

$$p3_{n+1}=0+p2_n * 2 * f_{as} * f_{ss}+p3_n * \left(f_{as}^3+6 * f_{as} * f_{ss} * f_{sd}\right)+\cdots$$

The similar algorithm can be applied to the rate of quadruplet $p4_{n+1}$ and more than 4 juxtaposed GFP$^+$ GSCs.

The simulation used the assumption that 7% GSCs became clones at the time of heatshock (Figure 3). The least squares fitting method was used to find the best fitted parameters by comparing the frequencies of total GFP$^+$ GSCs (i.e., the percentages of singlet, doublet, triplet, and quadruplet) from the simulation results at corresponding cell cycles and experimental data at 24, 36, 48, and 72 hrs (Table 1).

Acknowledgments

We thank David Glover, Liz Gavis, the Bloomington Stock Center, and the Developmental Studies Hybridoma Bank for reagents. This research was supported by the NIH (R01GM086481 to YMY). YMY is supported by the John D. and Catherine T. MacArthur Foundation. JC is partly supported by the Chicago Biomedical Consortium with support from The Searle Funds at The Chicago Community Trust.

References

1. Kai T, Spradling A. Differentiating germ cells can revert into functional stem cells in Drosophila melanogaster ovaries. Nature. 2004; 428:564–569. [PubMed: 15024390]
2. Brawley C, Matunis E. Regeneration of male germline stem cells by spermatogonial dedifferentiation in vivo. Science. 2004; 304:1331–1334. [PubMed: 15143218]
3. Cheng J, et al. Centrosome misorientation reduces stem cell division during ageing. Nature. 2008; 456:599–604. [PubMed: 18923395]
4. Sheng XR, Brawley CM, Matunis EL. Dedifferentiating spermatogonia outcompete somatic stem cells for niche occupancy in the Drosophila testis. Cell Stem Cell. 2009; 5:191–203.10.1016/j.stem.2009.05.024 [PubMed: 19664993]

5. Klein AM, Nakagawa T, Ichikawa R, Yoshida S, Simons BD. Mouse germ line stem cells undergo rapid and stochastic turnover. Cell Stem Cell. 2010; 7:214–224.10.1016/j.stem.2010.05.017 [PubMed: 20682447]
6. Nakagawa T, Nabeshima Y, Yoshida S. Functional identification of the actual and potential stem cell compartments in mouse spermatogenesis. Dev Cell. 2007; 12:195–206. [PubMed: 17276338]
7. Nakagawa T, Sharma M, Nabeshima Y, Braun RE, Yoshida S. Functional hierarchy and reversibility within the murine spermatogenic stem cell compartment. Science. 2010; 328:62–67.10.1126/science.1182868 [PubMed: 20299552]
8. Snippert HJ, et al. Intestinal crypt homeostasis results from neutral competition between symmetrically dividing Lgr5 stem cells. Cell. 2010; 143:134–144.10.1016/j.cell.2010.09.016 [PubMed: 20887898]
9. Aravin AA, Sachidanandam R, Girard A, Fejes-Toth K, Hannon GJ. Developmentally regulated piRNA clusters implicate MILI in transposon control. Science. 2007; 316:744–747.10.1126/science.1142612 [PubMed: 17446352]
10. Kiger AA, Jones DL, Schulz C, Rogers MB, Fuller MT. Stem cell self-renewal specified by JAK-STAT activation in response to a support cell cue. Science. 2001; 294:2542–2545. [PubMed: 11752574]
11. Tulina N, Matunis E. Control of stem cell self-renewal in Drosophila spermatogenesis by JAK-STAT signaling. Science. 2001; 294:2546–2549. [PubMed: 11752575]
12. Leatherman JL, Dinardo S. Zfh-1 controls somatic stem cell self-renewal in the Drosophila testis and nonautonomously influences germline stem cell self-renewal. Cell Stem Cell. 2008; 3:44–54. [PubMed: 18593558]
13. Leatherman JL, Dinardo S. Germline self-renewal requires cyst stem cells and stat regulates niche adhesion in Drosophila testes. Nat Cell Biol. 2010; 12:806–811.10.1038/ncb2086 [PubMed: 20622868]
14. Yamashita YM, Jones DL, Fuller MT. Orientation of asymmetric stem cell division by the APC tumor suppressor and centrosome. Science. 2003; 301:1547–1550. [PubMed: 12970569]
15. Yamashita YM, Mahowald AP, Perlin JR, Fuller MT. Asymmetric inheritance of mother versus daughter centrosome in stem cell division. Science. 2007; 315:518–521. [PubMed: 17255513]
16. Sheng XR, Matunis E. Live imaging of the Drosophila spermatogonial stem cell niche reveals novel mechanisms regulating germline stem cell output. Development. 2011; 138:3367–3376.10.1242/dev.065797 [PubMed: 21752931]
17. Yadlapalli S, Cheng J, Yamashita YM. Drosophila male germline stem cells do not asymmetrically segregate chromosome strands. J Cell Sci. 2011; 124:933–939.10.1242/jcs.079798 [PubMed: 21325028]
18. Boyle M, Wong C, Rocha M, Jones DL. Decline in Self-Renewal Factors Contributes to Aging of the Stem Cell Niche in the Drosophila Testis. Cell Stem Cell. 2007; 1:470–478. [PubMed: 18371382]
19. Wallenfang MR, Nayak R, DiNardo S. Dynamics of the male germline stem cell population during aging of Drosophila melanogaster. Aging Cell. 2006; 5:297–304. [PubMed: 16800845]
20. Jin Z, et al. Differentiation-defective stem cells outcompete normal stem cells for niche occupancy in the Drosophila ovary. Cell Stem Cell. 2008; 2:39–49. [PubMed: 18371420]
21. Yadlapalli S, Yamashita YM. Chromosome-specific nonrandom sister chromatid segregation during stem-cell division. Nature. 201310.1038/nature12106
22. Rogers GC, et al. Two mitotic kinesins cooperate to drive sister chromatid separation during anaphase. Nature. 2004; 427:364–370.10.1038/nature02256 [PubMed: 14681690]
23. Minestrini G, Harley AS, Glover DM. Localization of Pavarotti-KLP in living Drosophila embryos suggests roles in reorganizing the cortical cytoskeleton during the mitotic cycle. Mol Biol Cell. 2003; 14:4028–4038. [PubMed: 14517316]
24. Li C, et al. Collapse of germline piRNAs in the absence of Argonaute3 reveals somatic piRNAs in flies. Cell. 2009; 137:509–521.10.1016/j.cell.2009.04.027 [PubMed: 19395009]
25. Ameres SL, Zamore PD. Diversifying microRNA sequence and function. Nature reviews Molecular cell biology. 201310.1038/nrm3611

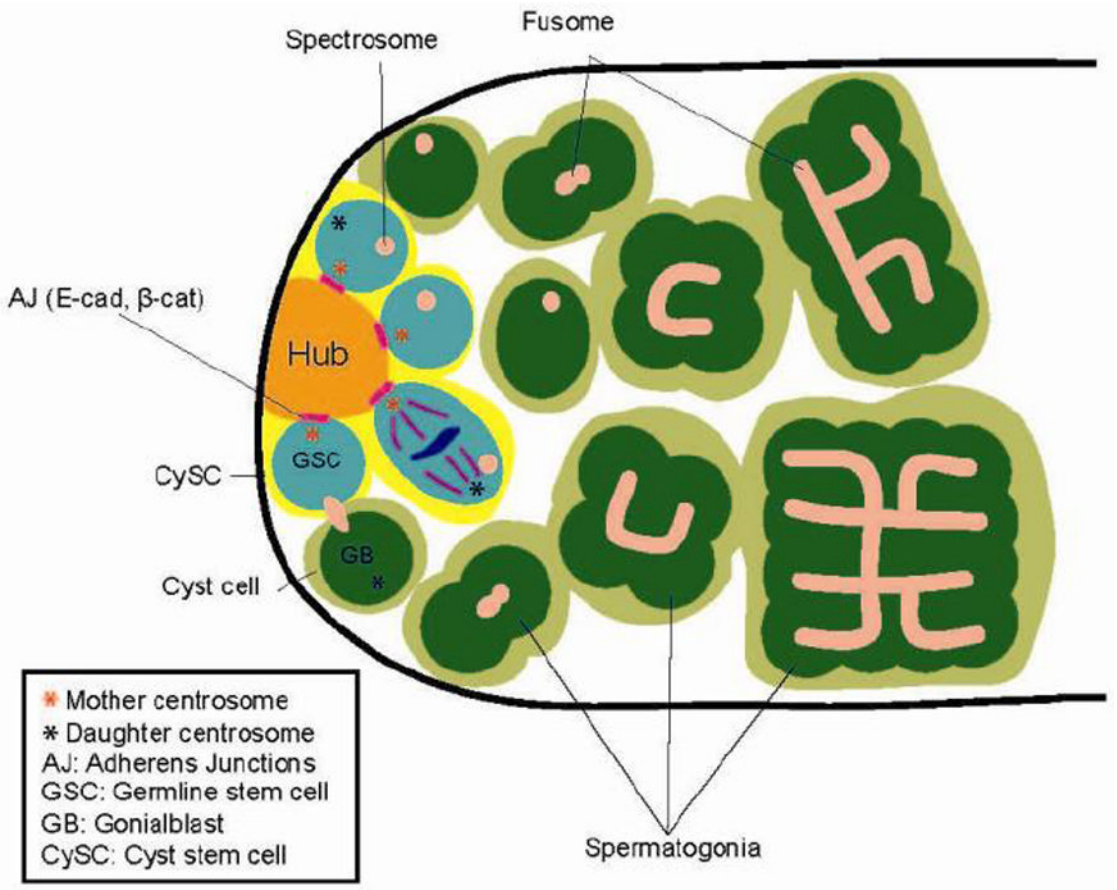

Figure 1. Anatomy of the *Drosophila* testicular niche

GSCs are attached to the hub cells through adherens junctions. GSCs divide asymmetrically by orienting the mitotic spindle perpendicular to the hub. Spindle orientation is prepared by stereotypical positioning of mother and daughter centrosomes. CySCs encapsulate GSCs, whereas CCs encapsulate GBs and spermatogonia. The spectrosome in GSCs branches to become a fusome as germ cells undergo transit-amplifying divisions.

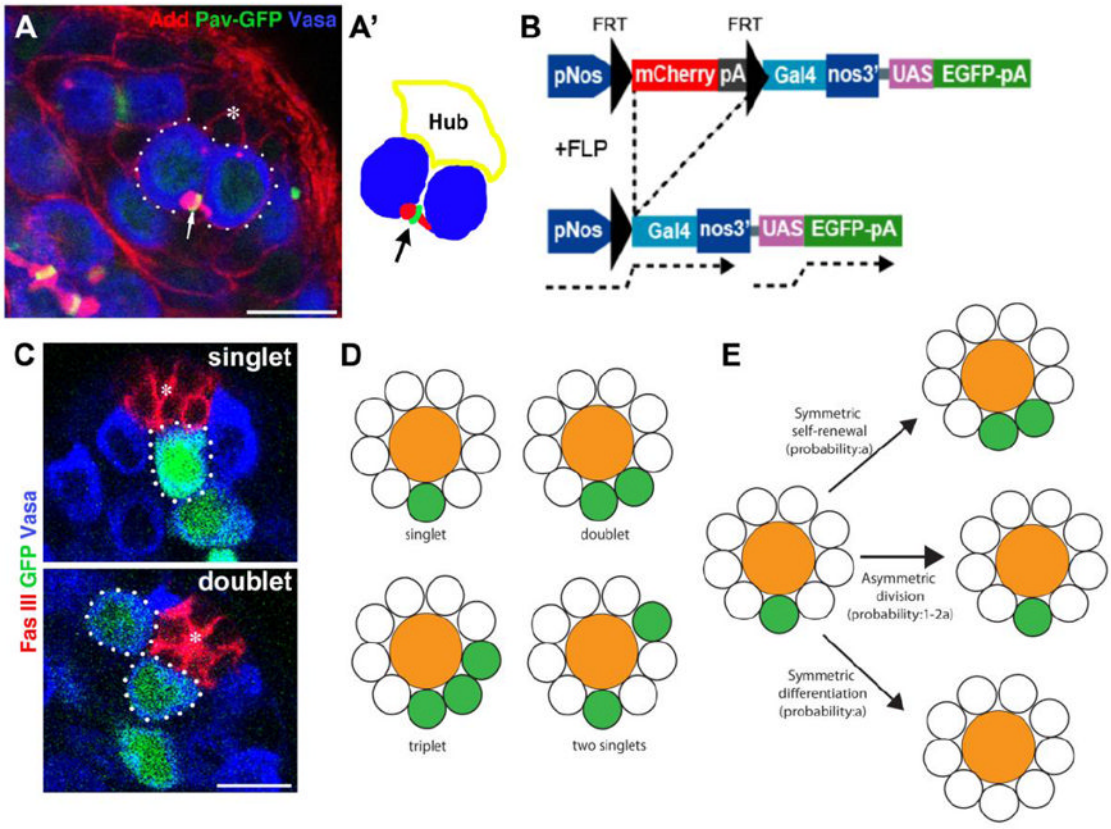

Figure 2. Experimental scheme to track the behavior of GSC divisions

A. An example of two GSCs (dotted lines) connected by the spectrosome (arrow). The hub is marked by the asterisk. Red: Add (adducin-like), spectrosome and fusome. Green: Pavarotti (Pav)-GFP, contractile ring/midbody. Blue: Vasa, germ cells. Drawing representation of A is shown in A'. Scale Bar: 10μm.

B. Transgene construct for clonal marking of GSCs. The Nos promoter and gal4 are separated by mCherry ORF followed by stop codons and a poly A sequence. mCherry-pA is flanked by FRT sequences, which can be removed by FLP-mediated recombination. Activated nos-gal4 drives the expression of UAS-GFP to mark the clones. Additional UAS transgene can be added to express the gene of interest in the clone.

C. Examples of singlet and doublet after heat shock–induced FLP-mediated activation of nos-gal4. These images were taken from the samples 24 hours post heatshock Red: Fas III (Fasciclin III, hub). Green: GFP (clones of active nos-gal4). Blue: Vasa, germ cells.

D. Definition of singlets and multiplets. When multiple GFP^+ GSCs are not juxtaposed, they were scored as multiple singlets.

E. The fate of singlets after symmetric self-renewal, asymmetric division, or symmetric differentiation.

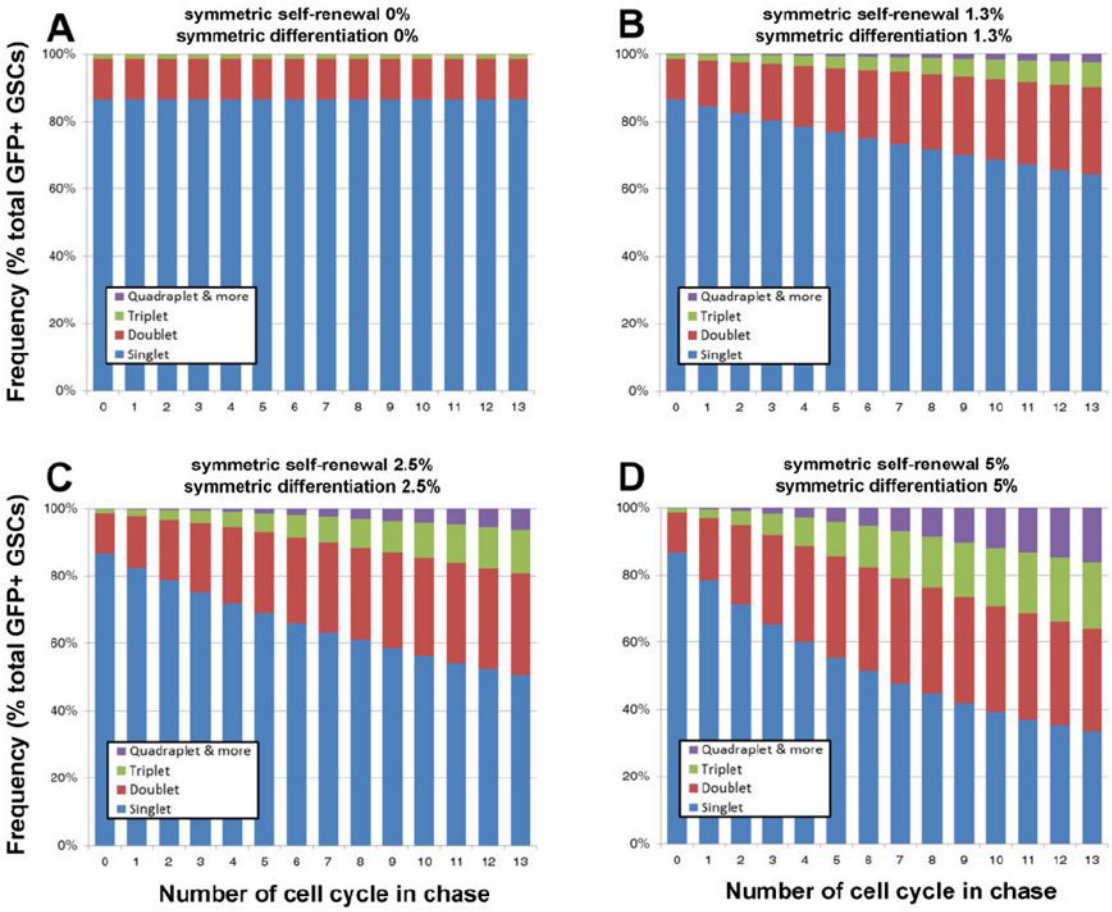

Figure 3. Simulation of changes in GFP$^+$ clones during the cell cycle

Simulation of how the distribution of singlets and multiplets will change during the cell cycles. A) Assuming 0% symmetric self-renewal and differentiation. B) Assuming 1.3% symmetric self-renewal and differentiation. C) Assuming 2.5% symmetric self-renewal and differentiation. D) Assuming 5% symmetric self-renewal and differentiation.

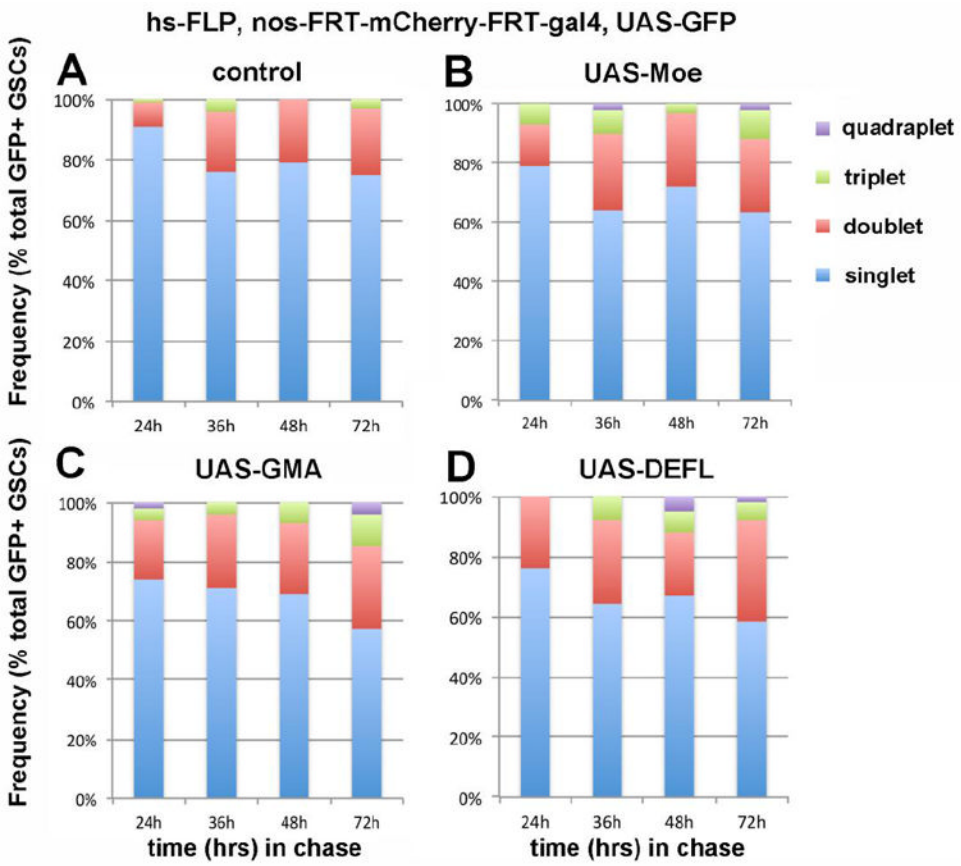

Figure 4. Changes in GFP$^+$ clones during the chase period after heat shock-induced FLP-recombination

A) Control flies: hs-FLP; nos-FRT-mCherry-pA-FRT-gal4, UAS-GFP. B) UAS-Moe-GFP was expressed in the clones. hs-FLP; nos-FRT-mCherry-pA-FRT-gal4, UAS-GFP, UAS-Moe-GFP. C) UAS-GMA was expressed in the clones. hs-FLP; nos-FRT-mCherry-pA-FRT-gal4, UAS-GFP, UAS-GMA. D) UAS-DEFL (E-cadherin tagged with GFP) was expressed in the clones. hs-FLP; nos-FRT-mCherry-pA-FRT-gal4, UAS-GFP, UAS-DEFL.

Table 1

Fitted asymmetric/symmetric GSC division rates

	12-hour cell cycle			16-hour cell cycle		
	Asymmetric division	Symmetric division		Asymmetric division	Symmetric division	
		Self-renewal	Differentiation		Self-renewal	Differentiation
WT	97.4%	1.3%	1.3%	96.2%	1.9%	1.9%
Moe	94.0%	3.0%	3.0%	92.4%	3.8%	3.8%
GMA	92.7%	3.7%	3.7%	90.3%	4.8%	4.8%
DEFL	91.8%	4.1%	4.1%	89.6%	5.2%	5.2%

Note that mitotic index of GSCs did not noticeably change upon expression of Moe or DEFL.